

# The Nature of the Complicated Fabric Textures: How to Represent in Primary Visual Cortex

J. L. Liu, L. Wang, B. Zhu, J. Zhou, W. D. Gao

**Abstract**—Fabric textures are very common in our daily life. However, the representation of fabric textures has never been explored from neuroscience view. Theoretical studies suggest that primary visual cortex (V1) uses a sparse code to efficiently represent natural images. However, how the simple cells in V1 encode the artificial textures is still a mystery. So, here we will take fabric texture as stimulus to study the response of independent component analysis that is established to model the receptive field of simple cells in V1. We choose 140 types of fabrics to get the classical fabric textures as materials. Experiment results indicate that the receptive fields of simple cells have obvious selectivity in orientation, frequency and phase when drifting gratings are used to determine their tuning properties. Additionally, the distribution of optimal orientation and frequency shows that the patch size selected from each original fabric image has a significant effect on the frequency selectivity.

**Keywords**—Fabric Texture, Receptive Filed, Simple Cell, Spare Coding.

## I. INTRODUCTION

SINCE the Nobel Prize winning work of Hubel and Wiesel it has been known that the selectivity of orientation, frequency and phase are the most important features of simple cells in the primary visual cortex (V1), which is also one of the most long standing hypothesis of neural representation for natural image [1]. At the level of primary visual cortex there is a large increase in the number of neurons. Hence, at this stage the idea of redundancy reduction cannot be motivated by a need for compression. However, the redundancy reduction principle is not limited to be useful compression only. More generally, it can be interpreted as a special form of density estimation where the goal is to model the statistics of the input by finding a mapping which transforms the data into a representation with statistically independent coefficients. In an influential paper, Olshausen and Field showed how the classical receptive fields of simple cells in V1 can be understood in a sparse coding framework [2]–[4], [5]. Yet numerous studies, many taking advantages of the fact that simple cells are the earliest in the visual pathway to encode input from both eyes, have demonstrated that receptive field properties are modified by visual experience during development [6]. In the research of

MacEvoy et al, they found that patterns of three shrew V1 activity evoked by superimposed equal-contrast gratings were predicted by the averages of patterns evoked by individual component gratings [7]. The success of the approach proposed to use multielectrode recording techniques to record neuronal activity at multiple sites in V1 and then use support vector machines to decode attended stimuli as stimulus contrast suggested that visual attention and stimulus contrast were represented by largely separable codes [8]. By analyzing the simultaneous responses of many cells in monkey visual cortex, Shriki et al pointed out that information about the orientation of visual stimuli can be extracted reliably from spike latencies on very short time scales [9]. The latest research suggested that information processing in primary sensory cortices could rely on different coding strategies across different layers [10].

Despite widespread research that natural images and scenes can be represented well by sparse coding that is coming from the response characteristics of simple cells in V1, there is no study that takes artificial fabric texture as stimuli to explore the features of simple cells. The purpose of this research is to investigate the mechanism of texture perception and explore the characteristics of receptive field of simple visual cell when various fabrics are used as visual stimuli. Textile fabrics are selected for research targets, because they can be systematically prepared through weaving machine by adjusting fiber materials, yarn thickness, yarn density, fabric structure and surface color. Moreover, everyone has a variety of memories about fabrics derived from experiences of viewing, touching, and wearing them[11].

## II. MODEL OF RECEPTIVE FIELD OF PRIMARY VISUAL CORTEX

### A. Model of Receptive Field

In this paper, we use independent component analysis to stimulate the receptive field of primary visual cortex. The generative model in ICA is defined by a linear transformation of the latent independent components [12]. If  $I(x,y)$  denotes the pixel grey-scale values in an image, or in practice, a small image patch. In ICA, an image patch is generated as a linear superposition of some features  $A_i$ ,

$$I(x, y) = \sum_{i=1}^m A_i(x, y) s_i \quad (1)$$

The  $S_i$  are coefficients that are statistically independent and non-gaussian when considered as random variables, which are the fundamental assumptions to define ICA model. These assumptions are enough to enable estimation of the  $S_i$ , if given a large enough sample of image patches.

J. L. Liu is with the Jiangnan University, Wuxi, 214122 China (phone: 86-510-85912007; fax: 86-510-85912009; e-mail: jian-li.liu@hotmail.com).

L. Wang, B. Zhu, J. Zhou, and W. D. Gao are with the Jiangnan University, Wuxi, 214122 China (e-mail: wangljn@163.com, zzb929@163.com, jzhou@jiangnan.edu.cn, gaowd3@163.com).

This project was supported by “National Natural Science Foundation of China” [Grant number 61203364], “China Postdoctoral Science Foundation” [grant number 20110490098], “Special Financial Grant from the China Postdoctoral Science Foundation” [Grant number 2012T50754].

As typical in linear models, estimation of the  $A_i$  is equivalent to determine the values of the  $W_i$  which give the  $S_i$  as outputs of linear feature detectors with some weights  $W_i$ ,

$$s_i = \sum_{x,y} W_i(x,y) I(x,y) \quad (2)$$

for each image patch. An important point to note is the relation between the feature vectors  $A_i$  and the feature detector weights  $W_i$ . The coefficients  $W_i$  are obtained by inverting the matrix of the  $A_i$ , which means that the  $A_i$  can be obtained by multiplying the  $W_i$  by the covariance matrix of the data. Thus,  $A_i$  and  $W_i$  have essentially the same orientation, location and frequency tuning properties. However, it is often the  $W_i$  that are more interesting, since they are the weights that are applied to the image to actually compute the  $S_i$ , and in neurophysiological modeling, they are more closely connected the receptive fields of simple vision cells [13], [14].

There are many different ICA algorithms which differ in the assumptions made and also in the optimization technique employed. The choice of the particular ICA algorithms used here was guided by a set of requirements that arise from the specific problem setting. We would like to use an ICA algorithm, which gives the ICA image basis the best chance for the comparison with other image representations. Therefore, we will use a pre-whitened ICA algorithm called FastICA [15], [12]. For the initialization with FastICA, we use the Gaussian non-linearity, the symmetric approach and a tolerance level of 10<sup>-5</sup>.

### B. Stimuli

In experiment, we resort to the dataset that includes 140 classical fabric images. This color image dataset is based on the collection of 70 samples that contain woven, knitted and jacquard fabrics provided by four different textile factories. For each fabric sample, we select two regions by a scanner called Epson GT20000. The scanning resolution and save format of each image is 300dpi and JPEG. Some of the 140 fabric images are demonstrated in Fig. 1.

During subsequent processing all images were transformed to gray ones. All images come at a resolution of 512×512 pixels. If each image circa 357 patches of size  $n \times n$  pixels are drawn at random locations, circa 50000 patches are gotten in total. For colorful images each is reshaped as an  $n \times n$  dimensional vector. In experiment, we respectively set the size of each selected patch as  $16 \times 16$  pixels and  $32 \times 32$  pixels for comparison. However, in the ICA program, the dimensionality of a data sample is thus reduced to 160 dimensions. To discuss the effect of patch size on the characteristics of primary visual receptive field extracted with ICA model, we will repeat the same analysis on a whole range of different patch sizes that cover  $2 \times 2$  pixels,  $4 \times 4$  pixels,  $8 \times 8$  pixels,  $16 \times 16$  pixels, and  $32 \times 32$  pixels.

The statistics of the average illumination in the image patches, the DC component, differs significantly from image to image. Therefore, the DC component was firstly separated from the patches before further transformation.

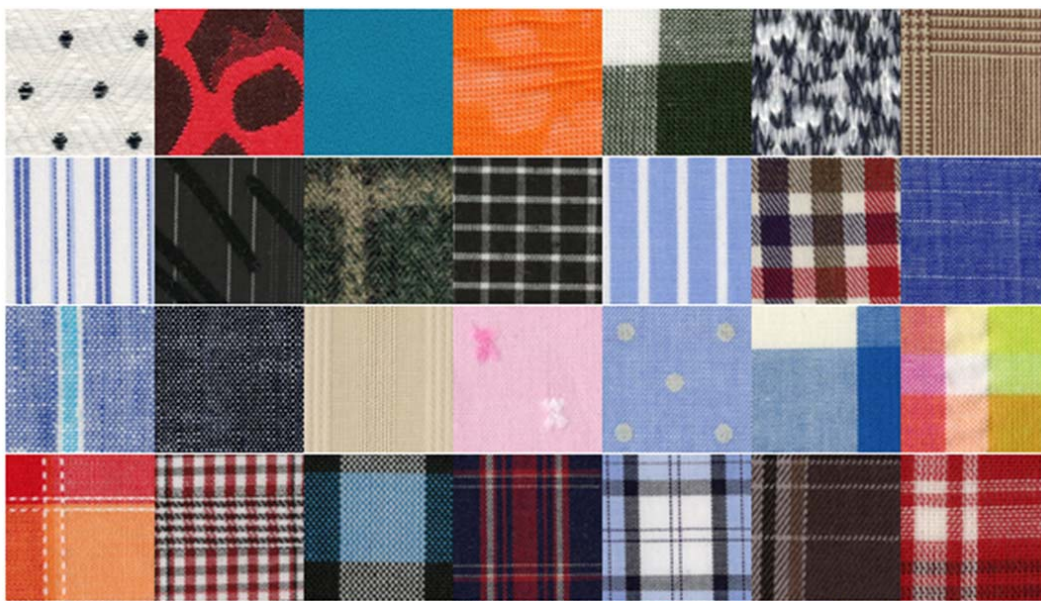


Fig. 1 Some fabric images

## III. RESULTS AND DISCUSSION

### A. Full Set of Receptive Fields Learned from Fabric Textures

In experiment, we randomly sampled 50000 image patches

of  $32 \times 32$  pixels, and applied canonical preprocessing to reduce the dimension to 160, which meant retaining 15.63% of the dimensions. To model the receptive fields of simple vision cells in primary visual cortex with fabric textures as stimuli, the

FastICA algorithm was implanted to calculate the receptive fields  $W_i$  shown in (2). The obtained receptive fields are shown in Fig. 2. To illustrate what has been learned from fabric textures, the receptive fields are coded so that the grey value of a pixel means the values of the coefficient at that pixel. Grey pixels mean zero coefficients. After converting the receptive fields to binary images by global thresholding, we can see much clearer details under higher contrast in Fig. 3.

Observing carefully, we can see that these receptive fields having interesting properties. Firstly, they are localized in space: most of the coefficients are practically zero outside of a small receptive field. Secondly, the receptive fields are also oriented: most of the orientations are similar to the ones of fabric textures.

Furthermore, they are multiscale in the sense that most of them seem to be coding for small structures whereas a few are coding for large structures.

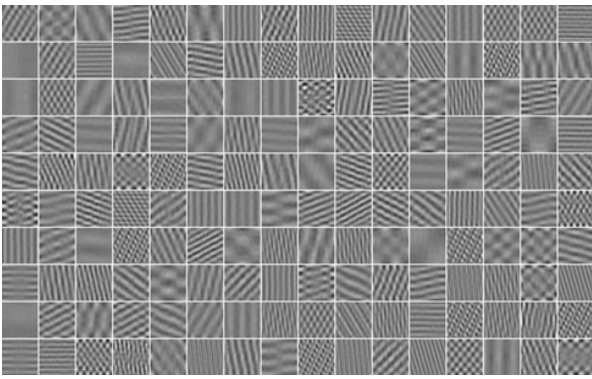


Fig. 2 Receptive fields of simple vision cells extracted from fabric textures

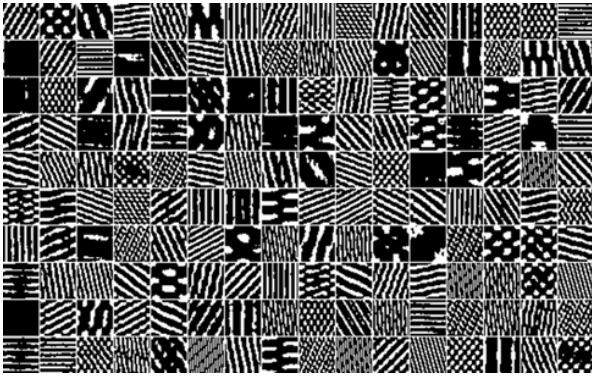


Fig. 3 Binary receptive fields as shown in Fig. 2

### B. The Tuning Properties of Receptive Fields

We can analyze the receptive fields  $W_i$  by looking at the responses when gratings, i.e., sinusoidal functions, are input to them. In other words, we create artificial images which are two dimensional sinusoids and compute the outputs  $S_i$ . Two sinusoidal functions used in here are

$$f_o(x, y) = \sin(2\pi\alpha(\sin(\theta)x + \cos(\theta)y)) \quad (3)$$

$$f_e(x, y) = \cos(2\pi\alpha(\sin(\theta)x + \cos(\theta)y)) \quad (4)$$

where  $\theta$  is the orientation, i.e., angle of the oscillation, the  $x$  axis corresponding to  $\theta=0$ . The parameter  $\alpha$  gives the frequency.  $x$  and  $y$  are the coordinates of one pixel in the image patch. The two functions give two oscillations in different phases.

If the number and values of orientations, frequencies, and phases are set, we can compute these functions for predefined orientations and frequencies. We normalize the obtained functions to unit norm. Then we calculate the dot-products of the receptive fields  $W_i$  with each of the gratings. We can then compute the optimal orientation and frequency by finding the  $\theta$  and  $\alpha$  that maximize the sum of the squares of the two dot-products corresponding to the sin and cos functions. That is to say the optimal orientation and frequency can be searched by solved the optimization problem described as

$$\begin{aligned} \max & \left( \left| W_i \cdot \sin(2\pi\alpha_j(\sin(\theta_k)x + \cos(\theta_k)y)) \right|^2 \right. \\ & \left. + \left| W_i \cdot \cos(2\pi\alpha_j(\sin(\theta_k)x + \cos(\theta_k)y)) \right|^2 \right) \end{aligned} \quad (5)$$

$$\text{s. t. } 0 \leq \theta_k \leq \pi, 0 \leq \alpha_j \leq n/2, 1 \leq k, j \leq 50 \quad (6)$$

where  $n$  is the number of columns of each image patch.  $x$  and  $y$  are the coordinates of the pixels in each image patch.

In neurophysiology, such analysis of tuning properties of visual cells is routinely performed with drifting gratings. However, we do not need to use drifting gratings in our work because the receptive fields learned from fabric textures are only mathematic models but neurobiological cells.

If the optimal frequency and orientation parameters are extracted for each receptive field by maximizing (5) subject to (6), the selectivity characteristics of orientation, frequency can be analyzed by changing one of the parameters in the grating. To analyze the selectivity to phase, we will simulate the response by simply taking the dot-product of  $W_i$  with gratings whose phase goes through all possible values, and still keeping the orientation and frequency at optimal values. In Fig. 4, the analysis for the first ten receptive fields in Fig. 2, i.e., the first ten receptive fields on the first row are shown. From left to right, the change in frequency, orientation and phase are demonstrated, as shown in Fig. 4. What we see is that all the cells are tuned to specific values of frequency, orientation, and phase: any deviation from the optimal values decreases the response.

It is also interesting to look at how the optimal orientations and frequencies are related to each other. This is shown in Fig. 5.

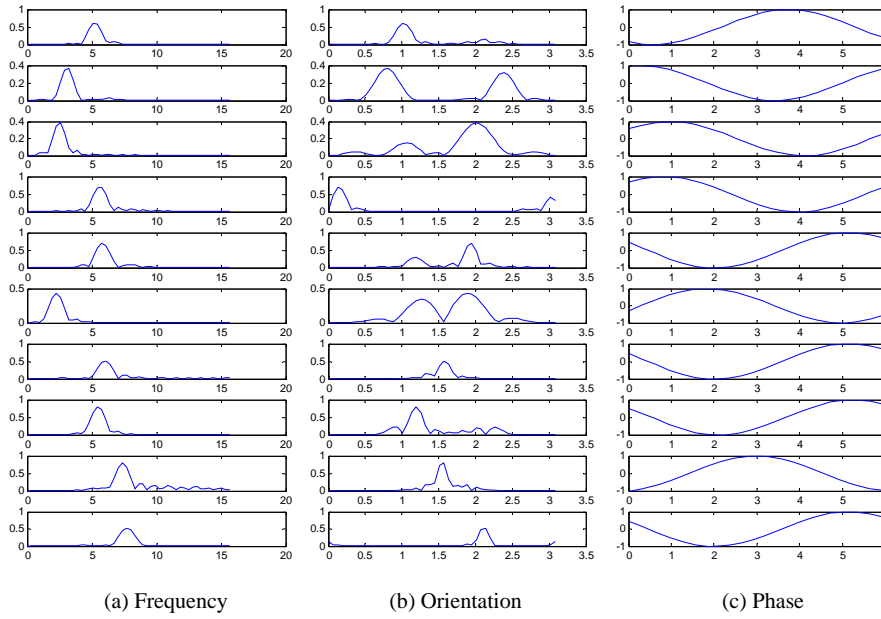


Fig. 4 Tuning curves of the first ten receptive fields in Fig. 2

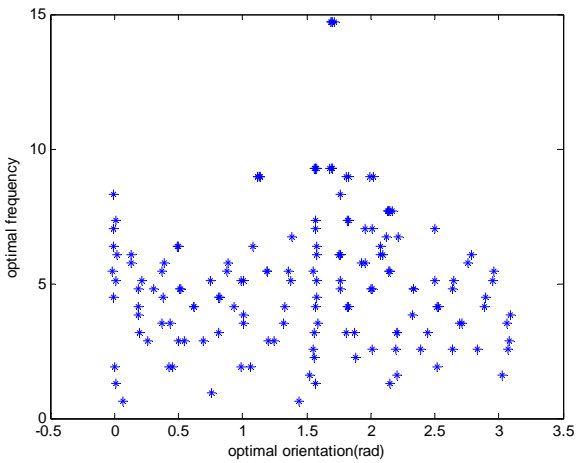


Fig. 5 Scatter plot of the frequencies and orientations of receptive fields

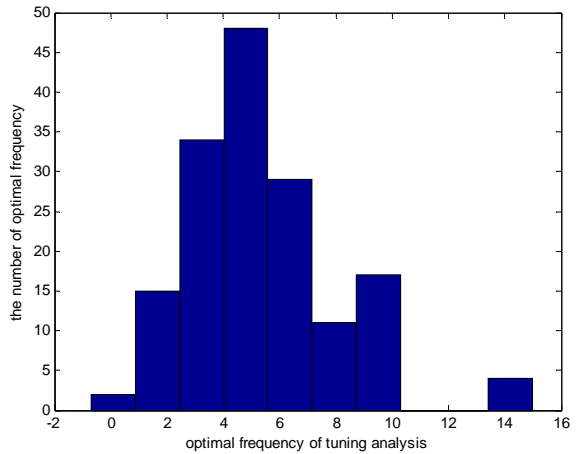


Fig. 6 Histograms of optimal frequencies

One can see that the 160 receptive fields cover all possible combinations of these variables, even though a few receptive fields have nearly the same optimal frequency and orientation. In Fig. 5, the highest frequencies are much lower (approx. Five cycles per patch) than the Nyquist frequency.

Another way of looking at the distributions is to plot the histograms of the two parameters separately, as shown in Figs. 6 and 7. Here we see again that most of the receptive fields have very high frequencies. The orientations are covered rather uniformly, but there are receptive fields with horizontal and vertical orientation. It is to say that fabrics have obvious stripes in horizontal and vertical directions. This is another expression of the directionality of fabric textures, which is one of the intrinsic characteristics because of the weaving processing.

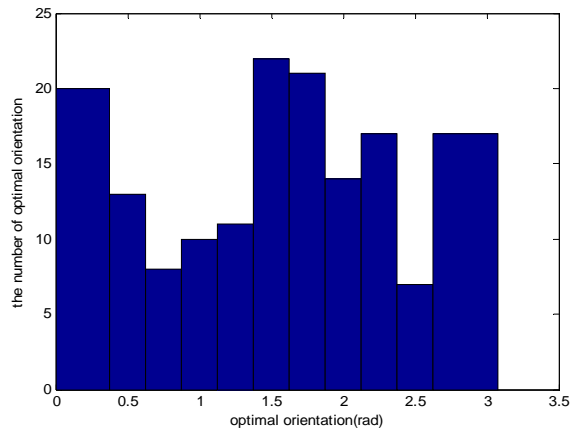
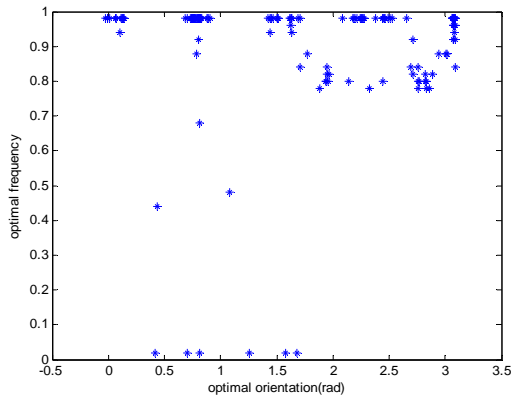


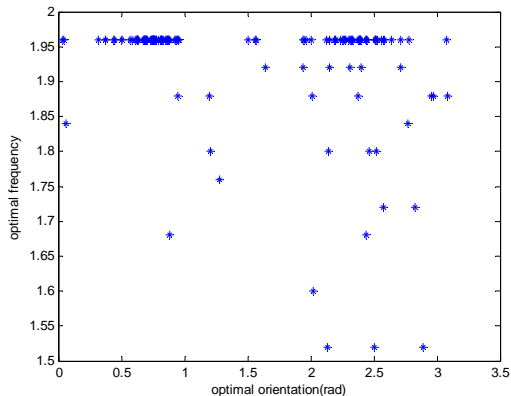
Fig. 7 Histograms of optimal orientations

### C. The Tuning Properties of Receptive Fields

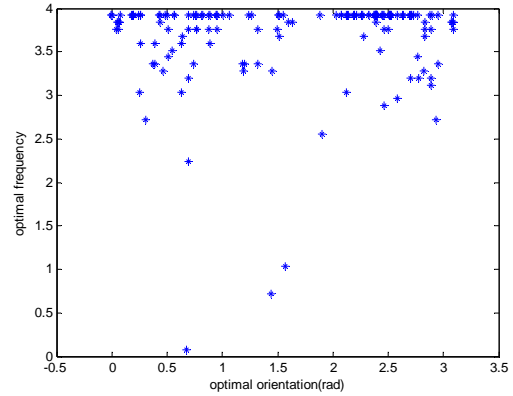
Our motivation to discuss the effect of patch size on the tuning characteristics of receptive fields is to explore the correlation of optimal frequencies and optimal orientations when different image sizes are selected. In experiment, we set the patch size to be 2 pixels  $\times$  2 pixels, 4 pixels  $\times$  4 pixels, 8 pixels  $\times$  8 pixels, 16 pixels  $\times$  16 pixels and 32 pixels  $\times$  32 pixels, respectively. One point can be easily found out from the following four figures is that the receptive fields become more and more anisotropic when the patch size increases from 2 pixels  $\times$  2 pixels to 32 pixels  $\times$  32 pixels, which is supported by the phenomenon that the distribution of optimal orientations becomes more discrete. Another conclusion can be induced is that the distribution of the optimal frequencies becomes more scattering and much evenner.



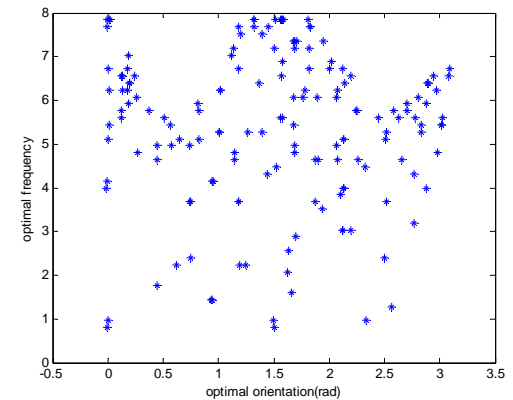
(a) The patch size is 2 pixels  $\times$  2 pixels



(b) The patch size is 4 pixels  $\times$  4 pixels



(c) The patch size is 8 pixels  $\times$  8 pixels



(d) The patch size is 16 pixels  $\times$  16 pixels

Fig. 8 The distribution of optimal orientations and optimal frequencies when different patch sizes are used

### IV. CONCLUSION

The selectivity of orientation, frequency and phase of simple cell in V1 are explored when fabric textures are used as stimulus. Experiment results indicate that the receptive fields of simple cells generated from independent component analysis have distinct orientation and frequency selectivity. The optimal orientation of each receptive field is determined by the dominant direction of the fabric textures. With the increase of patch size selected from each original fabric image, the optimal frequencies decided by drifting gratings become more scattering. Furthermore, the binary receptive fields include similar structure elements that existing in the original fabrics if the patch size is selected large enough.

### REFERENCES

- [1] J. Eichhorn, F. Sinz, and M. Bethge, "Natural image coding in V1: how much use is orientation selectivity?," *PLoS Comput. Biol.*, vol. 5, no. 4, p. e1000336, Apr. 2009.
- [2] B. a Olshausen and D. J. Field, "Natural image statistics and efficient coding.," *Network*, vol. 7, no. 2, pp. 333–9, May 1996.
- [3] P. O. Hoyer and A. Hyvarinen, "Sparse coding of natural contours," *Neurocomputing*, vol. 46, pp. 459–466, 2002.
- [4] J. Hurri and P. O. Hoyer, "Natural Image Statistics," 2009.

- [5] B. a Olshausen and D. J. Field, "Emergence of simple-cell receptive field properties by learning a sparse code for natural images.," *Nature*, vol. 381, no. 6583, pp. 607–9, Jun. 1996.
- [6] D. E. Mitchell, J. Kennie, D. S. Schwarzkopf, and F. Sengpiel, "Daily mixed visual experience that prevents amblyopia in cats does not always allow the development of good binocular depth perception.," *J. Vis.*, vol. 9, no. 5, pp. 22.1–7, Jan. 2009.
- [7] S. P. MacEvoy, T. R. Tucker, and D. Fitzpatrick, "A precise form of divisive suppression supports population coding in the primary visual cortex.," *Nat. Neurosci.*, vol. 12, no. 5, pp. 637–45, May 2009.
- [8] A. Pooresmaeili, J. Poort, A. Thiele, and P. R. Roelfsema, "Separable codes for attention and luminance contrast in the primary visual cortex.," *J. Neurosci.*, vol. 30, no. 38, pp. 12701–12711, Sep. 2010.
- [9] O. Shriki, A. Kohn, and M. Shamir, "Fast coding of orientation in primary visual cortex.," *PLoS Comput. Biol.*, vol. 8, no. 6, p. e1002536, Jan. 2012.
- [10] G. Basalyga, M. a Montemurro, and T. Wennekers, "Information coding in a laminar computational model of cat primary visual cortex.," *J. Comput. Neurosci.*, vol. 34, no. 2, pp. 273–83, Apr. 2013.
- [11] W. Lee and M. Sato, "Visual perception of texture of textiles," *Color Res. Appl.*, vol. 26, no. 6, pp. 469–477, Dec. 2001.
- [12] A. Hyvärinen and E. Oja, "Independent component analysis: algorithms and applications.," *Neural Networks*, vol. 13, no. 4–5, pp. 411–30, 2000.
- [13] L. Zhang and J. Mei, "Shaping up simple cell's receptive field of animal vision by ICA and its application in navigation system," *Neural Networks*, vol. 16, pp. 609–615, 2003.
- [14] A. Lörinicz, Z. Palotai, and G. Szirtes, "Efficient sparse coding in early sensory processing: lessons from signal recovery.," *PLoS Comput. Biol.*, vol. 8, no. 3, p. e1002372, Jan. 2012.
- [15] A. Hyvärinen, "Fast and robust fixed-point algorithms for independent component analysis.," *IEEE Trans. neural networks*, vol. 10, no. 3, pp. 626–34, Jan. 1999.